HHS Public Access

Author manuscript

Immunohorizons. Author manuscript; available in PMC 2022 October 20.

Published in final edited form as:

Immunohorizons. ; 4(5): 231–244. doi:10.4049/immunohorizons.2000020.

Differential Fuel Requirements of Human NK Cells and Human CD8 T Cells: Glutamine Regulates Glucose Uptake in Strongly Activated CD8 T Cells

Steven R. Presnell[*], **Henry K. Spear**[*], **Jerika Durham**[*], **Tyce Riddle**[*], **Austin Applegate**[*], **Charles T. Lutz**[*,†,‡]

[*]Department of Pathology and Laboratory Medicine, University of Kentucky, Lexington, KY 40536

[†]Department of Microbiology, Immunology, and Molecular Genetics, University of Kentucky, Lexington, KY 40536

[‡]The Markey Cancer Center, University of Kentucky, Lexington, KY 40536

Abstract

CD8 T cells and NK cells are the two major cytotoxic lymphocytes that carry out cell-mediated immunity and regulate other immune responses. However, we do not completely understand human CD8 T cell and NK cell metabolic requirements and they have not been compared in the same experiments. We activated human CD8 T cells by two anti–CD3/CD28 mAb methods, and we stimulated both CD8 T cells and NK cells with IL-12/IL-18. When glucose (Glc) could not be used, human CD8 T cells either died or became hypofunctional, depending upon the anti–CD3/CD28 activation method. In contrast, Glc starvation did not decrease the percentage of IL-12/IL-18–stimulated human NK cells that made IFN-γ. NK cells were relatively fuel resilient and used Glc, glutamine (Gln), fatty acid, or acetate to power IFN-γ expression. Surprisingly, strongly activated human CD8 T cells required Gln for glycolysis and Glc uptake. We showed that human CD8 T cells regulate Glc uptake by a novel mechanism related to the TXNIP pleiotropic protein. These conditions may be relevant to septic patients who have high blood Glc but low Gln. Under the conditions tested, Gln did not change human NK cell TXNIP expression. Our experiments reveal fundamental differences in human CD8 T cell and NK cell metabolism and the fuels needed for IFN-γ production.

INTRODUCTION

CD8 T cells and NK cells are the two major cytotoxic lymphocyte populations that carry out cell-mediated immunity and regulate other forms of immunity via cytotoxicity, cytokines, and other secreted molecules (1–5). Recent work has advanced our understanding of how metabolism influences T cell and NK cell development and function (6–13). Most work

Address correspondence and reprint requests to: Dr. Charles T. Lutz, University of Kentucky, 800 Rose Street, Room MS117, Lexington, KY 40536-0298. ctlutz2@uky.edu.

DISCLOSURES

The authors have no financial conflicts of interest.

in this field has used mouse CD4 T cells, with CD8 T cells and NK cells receiving less attention. Even less is known about human CD8 T cells and NK cells. To our knowledge, no work has yet been reported comparing function of these cells in the same context. We addressed this knowledge gap by studying human cytotoxic lymphocytes in parallel under similar conditions.

Culture media nutrient concentrations have been optimized for vigorous responses. Compared with typical culture media, glucose (Glc) and glutamine (Gln) concentrations are low in blood and even lower in tissues. Nutrients can be even lower at infected sites (14) and in the tumor microenvironment (8, 15–17). An interesting situation is found in sepsis, which is characterized by very high blood Glc and low blood and tissue Gln (18–21). To study lymphocyte function under nutrient-poor conditions, many investigators have limited fuels for a few hours to a day. We chose to expose human CD8 T cell and NK cells to low nutrient levels for 2 d. This relatively long nutrient deprivation is justified by the observation that tissue-resident memory T cells and their progeny persist for long periods in infected tissues (22). Furthermore, tumor-infiltrating CD8 T lymphocyte number is maintained for at least 6 d, despite blockade of new immigrants (23). Thus, CD8 T cells and their progeny are exposed to the tumor microenvironment for many days (23).

T cells use a variety of fuels in different circumstances, but multiple investigators showed that mouse effector T cell function requires extracellular Glc and glycolysis (6, 7, 9, 10). However, one report concluded that human CD4 and CD8 IFN-γ production was independent of Glc concentration (24). Two competing paradigms explained why T cell IFN-γ production requires glycolysis. In the translation blockade hypothesis, GAPDH, when not involved in glycolysis, binds to the 3′ untranslated region of IFN-γ mRNA and prevents its protein synthesis (6). In the epigenetic hypothesis, low glycolysis depletes cytosolic acetyl-CoA, reducing histone acetylation at the *IFNG* gene and inhibiting transcription (7). Both mechanisms were supported by experiments with mice but have not been explored in human CD8 T cells. Despite their Glc addiction, effector T cell functions also require Gln. Several mechanisms have been tested in mouse T cells, but not in human CD8 T cells.

Human NK cells can be divided into low-cytotoxicity $CD56^{bright}$ cells and highly cytotoxic $CD56^{dim}$ cells (1). These cells have been characterized as “immature” and “mature,” respectively, but differ in turnover and sensitivity to various stimuli. Under our study conditions, both $CD56^{bright}$ and $CD56^{dim}$ NK cells respond vigorously to IL-12/IL-18 monokines. Although metabolic requirements of these two NK cell populations have been studied in the context of unpurified human mononuclear preparations (13, 25), we are not aware of any study looking at the fuel requirements of purified human NK cells.

For the current study, we compare human CD8 T cells and NK cells in the same assays under similar conditions. We find that the T and NK cytotoxic lymphocytes differ markedly in their metabolic requirements. We also investigate possible metabolic differences in T cell activation. We test T cells under different anti–CD3/CD28–activating conditions and find markedly different responses to Glc deprivation. Moreover, different cytokines are regulated by distinct mechanisms in Glc-depleted human CD8 T cells. Finally, we uncover a novel

mechanism by which Gln regulates Glc use in activated human CD8 T cells. Our work has important implications for effector human CD8 T cell and NK cell function in nutrition-poor environments, including infected tissues and the tumor microenvironment.

MATERIALS AND METHODS

Human subjects and flow cytometry

In accordance with the Declaration of Helsinki (modified in 2008), all protocols were approved by the Institutional Review Board of the University of Kentucky, Lexington, KY. The male and female adult subjects were aware of the design and purpose of the studies and signed consent forms. Peripheral blood was collected by venipuncture and mixed with either human NK or CD8 T Rosette Sep Ab mixture (Stem Cell Technologies) as instructed by the manufacturer, diluted (1:1 v/v) with wash solution (Dulbecco PBS [without Ca^{2+} or Mg^{2+}; Sigma-Aldrich] with 2% FBS [HyClone]). Following centrifugation on either Histopaque-1077 (Sigma-Aldrich) or Lymphoprep (Stem Cell Technologies) at 300 × *g* for 20 min, brake off, interface cells were washed in wash solution and washed again in media (Glc and Gln defficient RPMI-1640 [MP Biomedicals] with 1× nonessential amino acids without Gln [catalog no. M7145; Sigma-Aldrich], 1× penicillin-streptomycin, and 10% dialyzed FBS [catalog no. F0392; Sigma-Aldrich]). Approximately 200,000 CD8 T or NK cells (average purity, 90–95%) were resuspended in 0.15 ml of media with Glc and Gln added, as indicated, in 96-well polystyrene plates and incubated in 5% CO_2 at 37°C. In some cases, the wells were coated with 0.15 ml of anti-human CD3 (clone OKT3, 1.0 μg/ml in PBS; eBioscience) for 2 d at 4°C, and washed once with PBS before cells were added. To these wells, soluble anti-human CD28 (clone CD28.2; eBioscience) was added to cells (final concentration 5 μg/ml). In other cases, human T-activator Dynabeads (Life Technologies), which have bound mAb to human CD3 and CD28, were added to CD8 T cells at 1:1 bead/cell ratio. No exogenous IL-2 was added. NK and CD8 T cells were incubated for a total of 42 h, with IL-12/IL-18 (10 and 100 ng/ml respectively; BioLegend) added in the final 24 h. In some experiments, PMA/A23187 (25 and 250 ng/ml, respectively; Sigma-Aldrich) was added 5 h before harvest. For flow cytometry analysis, 1× brefeldin A and monensin (BioLegend) was added 3 h before harvest. At harvest, cells were added to FACS tubes, cells were stripped from beads by drawing up cells 40 times in a pipette tip, and beads were removed with a magnet. Cells were washed with PBS and incubated with 0.1 ml of 1:1000 diluted eFluor780 viability dye (eBioscience) in PBS for 30 min at room temperature, washed with FACS buffer, then surface stained for 30 min on ice. For CD8 T cell analysis, fluorescent mAb were specific for CD8 (RPA-T8), CD45RA (HI100), CCR7 (3D12); for NK cells, CD3 (UCHT1), CD16 (B73.1), CD56 (HCD56). After surface staining, cells were washed with 20 mM HEPES and 150 mM NaCl (Sigma-Aldrich) (pH 7.5), then with 50 μl of this buffer with 5 mM calcium chloride (annexin buffer) and Annexin PE-Cy7 for 15 min on ice. Cells were washed with annexin buffer and fixed with 2% formaldehyde dissolved in annexin buffer 15 min. Cells were then washed twice with 1× permeabilization buffer (eBioscience), and stained with mAb specific for IFN-γ (45.15), TNF-α (Mab11), or GzmB (GB11), then washed with FACS buffer and fixed in 2% formaldehyde in PBS. Gating strategy is described in Supplemental Fig. 1.

For Glc uptake experiments, cells were plated in media as described above for 39 h, washed in media with 1% dialyzed FBS, and incubated for 3 h in 0.1 mM 2-[*N*-(7-nitrobenz-2-oxa-1,3-diazol-4-yl)amino]-2-deoxy-D-glucose (2-NBDG; Cayman Chemical) in media with 1% dialyzed FBS. Cells were harvested, treated with eFluor 780 for dead cell discrimination, surface stained as described above, and immediately underwent flow cytometry. For mitochondrial content analysis, PBMCs were stained with mAb to cell surface proteins and treated with 10 nM Mitoview Green (Biotium) for 1 h. In these experiments, $CD3^+$ $CD4^-$ $CD45RA^-$staining identified $CD3^+$ $CD4^-$ $CDRA^-$ CD8 T cells; $CD56^{dim}$ and $CD3^-$ staining identified $CD56^{dim}$ NK cells. The median fluorescence intensity (MFI) of the Mitoview Green peak was subtracted from the MFI of the unstained sample to determine relative fluorescence. All mAb were from BioLegend, eBioscience, or BD Biosciences. Flow cytometry was carried out with an LSR II (BD Biosciences), and data were analyzed with FlowJo software.

Chemicals, ATP, and mRNA quantitation

Oligomycin A (10 mg/ml stock dissolved in 100% DMSO; Sigma-Aldrich), etomoxir (ETO; 40 mM stock dissolved in water; Sigma-Aldrich), or sodium acetate (Sigma-Aldrich) was added to a final concentration indicated, at either 18 h before harvest (oligomycin), or through the entire incubation (ETO, acetate). Oligomycin activity was confirmed by a loss of oxygen consumption rate (OCR) through Seahorse analysis of CD8 T cells. ATP from 200,000 cells was measured with an ATP-Lite Luminescence Assay Kit (Perkin-Elmer) using instructions from the manufacturer. Luminescence for each condition was measured in duplicate (80,000 cells per test), and a standard curve was prepared as instructed.
For mRNA analysis, total RNA was prepared from 200,000 cells using an RNeasy UCP Micro Kit (Qiagen), and converted to cDNA using random hexamer priming with a High-Capacity cDNA Reverse Transcription Kit (Applied Biosystems), using instructions from the manufacturer. Quantitative PCR was carried out with the following primers: Housekeeping RNA controls are as follows: PGK-1 s: 5′-GCT GGA CAA GCT GGA CGT TA-3′ as: 5′-AGC CTT AAT CCT CTG GT-3′; GUSBs: 5′-GAA AAT ATG TGG TTG GAG AGC TCA TT-3′ as: 5′-CCG AGT GAA GAT CCC CTTT TTA-3′; SDHA s: 5′-TGG GAA CAA GAG GGC ATC TG-3′ as: 5′-CCA CTG CAT CAA ATT CAT G-3′; INTS-4 s: 5′-GCA GCT CCA TGA AAG AGG AC-3′ as: 5′-ACC CAG ATA AGC TGG ACT GC-3′; RPLP0 s: 5′-GGC GAC CTG GAA GTC CAA CT-3′, as: 5′-CCA TCA GCA CCA CAG CCT TC-3′; U2s: 5′-TGG AGC AGG GAG ATG GAA TA-3′ as: 5′-CGT TCC TGG AGG TAC TGC AA-3′; U6 s: 5′-CGC TTC GGC AGC ACA TAT AC-3′ as: 5′-CGA ATT TGC GTG TCA TCC TT-3′; and 7SL s: 5′-ATC GGG TGT CCG CAC TAA GTT-3′ as: 5′-CAG CAC GGG AGT TTT GAC CT-3′.Eight controls were used for IFN-γ, TNF-α, GzmB quantitation and all except U2 for thioredoxin-interacting protein (TXNIP) mRNA quantitation. Target mRNAs are as follows: IFN-γ s: 5′-CCA GAG CAT CCA AAA GAG TGT G-3′ as: 5′-ATT GCT TTG CGT TGG ACA TTC A-3′; TNF-α: s: 5′-CCA GGG ACC TCT CTC TAA TCA-3′ as: 5′-GGC TAC AGG CTT GTC ACT C-3′; GzmB, s: 5′-TGC AGG AAG ATC GAA AGT GCG-3′ as: 5′-GAG GCA TGC CAT TGT TTC GTC-3′; and TXNIP, s: 5′-TGG ATG TCA ATA CCC CT-3′ as: 5′-ATT GGC AAG GTA AGT GTG GC-3′. All primers (Integrated DNA Technologies or Sigma-Aldrich) had 90 and 110%, amplification efficiencies and amplicons of the correct size. The program used

was denaturation at 95.0 ℃ for 5 s, annealing at 64 or 66.0 ℃ for 10 s, and extension at 72 ℃ for 30 s, using 1× SYBR green mix (Bioline). All sample volumes were 10 μl and amplified in triplicate reactions on a Bio-Rad CFX96 real-time system. The cycle quantification value was determined from amplification curves using Bio-Rad CFX manager software. For analysis of test mRNA, the fold change was determined from the geometric mean of housekeeping control RNAs using the formula $2^{(-[\text{Cq target} - \text{Cq geo mean HK}])}$.

Seahorse

Cultured cells were washed in 1× Seahorse XF RPMI media (provided by the manufacturer) with the appropriate amount Glc, Gln, and ETO (Sigma-Aldrich). Six hundred thousand CD8 T (with beads) or NK cells were resuspended in 0.2 ml of this media and added to wells of an eight or 96-well Seahorse plate; Cell-Tak was not used. Microscopic examination showed confluent cells on the Seahorse plate at the end of each experiment, but we cannot rule out some cell loss. It is possible that our approach might have produced extracellular acidification rate (ECAR) and OCR results different from those collected using Cell-Tak. Because of the excessive number of cells needed to receive a signal above background, all experiments reported had only one well of 600,000 cells per donor analyzed. Assays were performed with either a XF8 or XF96 Analyzer (Seahorse Bioscience); three measurements were averaged to calculate ECAR and OCR.

Statistical analysis

Means were compared using paired, two-tailed Student *t* tests, except when *F*-statistics indicated that groups had dissimilar variances. Where noted in the figure legends, data were logarithmically transformed, allowing Student *t* testing. Error bars represent SEM.

RESULTS

Activation conditions determine human CD8 T cells response to Glc

We studied human CD8 T cells and NK cells, the two major classes of cytotoxic lymphocytes that secrete IFN-γ and are important in cell-mediated immunity (1, 5, 26). Human CD8 T cells were isolated from fresh blood and were activated under a commonly-used condition; anti-CD3 mAb was bound to the surface of polystyrene plates and soluble anti-CD28 mAb was added with isolated blood CD8 T cells for 2 d. We will refer to this condition as “plate activated.” Alternatively, we activated human CD8 T cells from the same subjects with anti-CD3 and anti-CD28 mAb that were both bound to Dynabeads. We will refer to this latter condition as “bead activated.” To mimic conditions in which human lymphocytes are exposed to macrophages and dendritic cell monokines, we added IL-12 and IL-18 (10 and 100 ng/ml, respectively) in the final 24 h. We chose these conditions because plate-activated CD8 T cell IFN-γ production required both Ab activation and monokine stimulation (Supplemental Fig. 2). Although bead-activated CD8 T cells produced cytokines in response to anti–CD3/CD28 alone, production was greatly boosted with IL-12/IL-18 monokines. $CD56^{bright}$ and $CD56^{dim}$ NK cell IFN-γ production absolutely required IL-12/18 stimulation (Supplemental Fig. 2). To compare the two anti–CD3/CD28 T cell activation methods with each other and with NK cells, all cultures were treated with IL-12/18 for the final 24 h. Culture media consisted of Glc- and Gln-free RPMI-1640 and

dialyzed calf serum, which allowed us to manipulate these nutrients over a wide range. Human serum Glc ranges from 3.9 to 7.2 mM (27). Glc concentration has been estimated to range from undetectable to 1.3 mM in experimental tumors (8, 15) and also is low in human bacterial meningitis (14). We measured intracellular cytokines and GzmB by flow cytometry.

As expected, $CD45RA^-$ memory CD8 T cells made considerable cytokines and GzmB under these conditions, but $CD45RA^+$ naive CD8 T cell responses varied considerably among research subjects and were often very low (data not shown). Therefore, we focused on memory T cells. Anti–CD3/CD28 bead activated human CD8 T cells produced much more IFN-γ, TNF-α, and GzmB than did plate-activated CD8 T cells. Fig. 1A shows a typical result and Fig. 1B–D show subject averages. In Fig. 1B–D (left side), percentage-expressing cells are shown at 11 mM Glc. For ease of comparison, normalized values (right side) are shown at other concentrations. Under both anti–CD3/CD28 activation conditions, human CD8 T cell responses were very sensitive to Glc concentration. Most anti–CD3/CD28 plate–activated, IL-12/IL-18–stimulated human CD8 T cells showed signs of apoptosis or late-stage cell death in ≤0.1 mM Glc (Fig. 1E). To confirm that loss of human CD8 T cell responses was due to a main effect on glycolysis, we replaced Glc with galactose (Gal) as the major carbon source in media. Gal is not efficiently used for glycolysis in most cell types. Like low Glc concentrations, the replacement of Glc with Gal greatly reduced cytokine and GzmB responses by bead-activated human CD8 T cell and killed plate-activated CD8 T cells. The great majority of bead-activated CD8 T cells remained viable at all Glc concentrations (Fig. 1E). As an additional test of viability and function, we activated human CD8 T in low Glc with anti–CD3/CD28 beads, and then stimulated cells with PMA and calcium ionophore. With this nonphysiological stimulus, human CD8 T cell cytokine production was intact at all Glc concentrations tested (Fig. 1F). Together, these findings indicated that human memory CD8 T cells, like mouse T cells (6, 7, 10), required glycolysis for optimal cytokine and GzmB responses. Our findings contrast with another group, which concluded that human CD8 T cells do not require Glc for IFN-γ production (24). However, that group lowered, but did not eliminate, Glc in their culture media. Another notable feature of our work is that seemingly small differences in anti–CD3/CD28 activation yielded major differences in the responses to IL-12/IL-18 monokines. These differences in signal strength or quality caused human CD8 T cells either to undergo apoptosis or to become hyporesponsive in low Glc.

Human NK cells do not require Glc

Like mature CD8 T cells, mature NK cells are cytotoxic lymphocytes that produce IFN-γ and other cytokines. We wished to compare CD8 T cell results with those of isolated human NK cells, usually tested from the same research subjects in the same experiments with varying Glc concentrations. We stimulated NK cells with IL-12/IL-18 for the final 24 h of the 2 d culture, which elevated NK cell metabolism (nearly 3-fold increase in glycolysis and a 67% increase in O_2 consumption), but did not change $CD56^{bright}$ and $CD56^{dim}$ ratios (data not shown). Under these conditions, NK cells expressed abundant IFN-γ and GzmB. TNF-α levels varied between donors and were often low-level. To accurately quantify decreases in NK cell responses, we focused on IFN-γ and GzmB. When we reduced Glc concentration,

the percentage of immature $CD56^{bright}$ and mature $CD56^{dim}$ NK cells expressing IFN-γ and GzmB remained almost constant. Replacement of Glc with Gal also had minimal effects on the percentage responding NK cells (Fig. 1B, 1D). GzmB MFI was only mildly sensitive to low Glc or to Gal (Supplemental Fig. 3A). We note that although substitution of Gal for Glc only slightly reduced or did not affect the percentage responding $CD56^{bright}$ and $CD56^{dim}$ NK cells, respectively, the amount of IFN-γ made per cell was diminished to ~40% of control high Glc conditions (Supplemental Fig. 3B). Collectively, these results showed that IL-12/IL-18–stimulated human NK cell continued to express IFN-γ and GzmB in the absence of exogenous Glc. As expected, human NK cells also responded to PMA and calcium ionophore in low Glc (data not shown). Our experiments illuminated a major difference between human cytotoxic lymphocytes: CD8 T cells strictly required glycolysis for responses and/or survival, whereas NK cell function was much less dependent on glycolysis. This suggested that human NK cells may be effective when Glc is low, such as in the tumor microenvironment or infectious sites (8, 14–16).

Low Glc affects human CD8 T cell cytokines at the level of mRNA or protein

We wished to explore mechanisms of how Glc starvation inhibited effector molecule production in human CD8 T cells. We measured mRNA in anti–CD3/CD28 bead–activated, IL-12/IL-18–stimulated human CD8 T cells under different Glc levels. Metabolism changes gene expression, so we measured cytokine and GzmB expression, standardized against the geometric mean of eight control RNAs, including mRNAs and small nuclear RNAs (Materials and Methods). IFN-γ and GzmB mRNA levels declined with decreasing Glc and fell to ~10% of “full” levels at 0.1 mM Glc (Fig. 2A), paralleling the decline in protein levels (Fig. 1B–D). We conclude that Glc starvation reduces *IFNG* and *GZMB* transcription or RNA stability. In contrast, TNF-α mRNA levels declined modestly in low Glc. At 1.1 mM Glc, TNF-α mRNA had not changed (Fig. 2A) despite a >80% loss of TNF-α protein (Fig.1C). We conclude that Glc starvation acted mainly to decrease human CD8 T cell TNF-α translation or protein stability, rather than transcription. As expected, human NK cell IFN-γ and GzmB mRNA, and low-level TNF-α mRNA, did not significantly decline, even at 0.01 mM Glc (Fig. 2B). We are extending our study of these interesting differences.

Human CD8 T and NK cell metabolism in low Glc

To understand how Glc deprivation changed metabolism, we examined acid excretion rates (ECAR, a measure of glycolysis) and OCR (a measure of OxPhos). As above, we activated human CD8 T cells with anti–CD3/CD28 and stimulated them with IL-12/IL-18, and we stimulated human NK cells with IL-12/IL-18. The Glc concentration present at culture initiation was reproduced in the Seahorse instrument. Correlating with the strength of signaling, bead-activated CD8 T cells had more glycolysis and consumed more O_2 than did plate-activated T cells or NK cells (Fig. 3A, 3B). As expected, both CD8 and NK cells reduced glycolysis as Glc concentrations were lowered. CD8 T cell OCR gradually declined as Glc concentration fell. NK cells maintained OCR, suggesting that they did not require Glc to fuel OxPhos. Because metabolism was likely to affect energy level, we measured cellular ATP levels. At 11 mM Glc, anti–CD3/CD28 bead–activated, IL-12/IL-18–stimulated CD8 T cells had higher cellular ATP levels than did NK cells (Fig.3C). As Glc concentrations were lowered or as Gal was substituted for Glc, CD8 T cell ATP levels fell to less than half of

levels in standard culture media (Fig. 3C). This ATP loss in human CD8 T cells took place in a 2-d culture. Others have found that a 5-h Glc starvation did not reduce mouse CD8 T cell ATP levels (9). Distinct from CD8 T cells, human NK cells maintained a nearly constant level of ATP (Fig. 3C). These results suggested that human CD8 T cells heavily relied on glycolysis for energy, whereas human NK cells consumed other fuels for cellular energy. Although human CD8 T cellular ATP fell, at 0.1 mM Glc, ATP levels were moderate (Fig. 3C) and O_2 consumption was high (Fig. 3B) compared with human NK cells. Yet this Glc concentration abrogated IL-12/IL-18–stimulated CD8 T cell cytokine and GzmB production, with modest effect on NK cell cytokine and GzmB expression (Fig. 1B–D).

Human CD8 T cell effector responses require both Glc and Gln

Given that NK cells maintained ample IFN-γ expression, O_2 consumption, and cellular ATP despite low Glc, we explored if human cytotoxic cells use Gln. This was important because human carcinomas deplete Gln more than any other amino acid (16, 17), and sepsis is characterized by low blood Gln (20, 21). We activated human CD8 T cells with anti–CD3/CD28 and stimulated them with IL-12/IL-18 while varying both Glc (11, 1.1, or 0.1 mM) and Gln (2.0 or 0.02 mM) concentrations. As before, human CD8 T cells required high Glc levels for IL-12/IL-18–stimulated cytokine production or for survival, depending upon the activation conditions (Fig. 4A–C). With relatively weak anti–CD3/CD28 plate activation, low Gln did not influence CD8 T cell viability when Glc ≥1.1 mM (Fig. 4C). However, bead-activated human CD8 T cells required Gln to respond to IL-12/IL-18 (Fig. 4A, 4B). At 0.02 mM Gln, bead-activated CD8 T cell TNF-α and IFN-γ production was only ~20% of that at 2 mM Gln, even when Glc was high (11 mM). We concluded that strongly activated human CD8 T cells required both Glc and Gln for robust cytokine responses. In contrast, most human $CD56^{bright}$ and $CD56^{dim}$ NK cells produced IFN-γ at all Glc and Gln concentrations tested (Fig. 4A). There was some decline the amount of IFN-γ produced per NK cell (Supplemental Fig. 3C), even while the percentage responding NK cells remained high. It is worth noting that despite their developmental and functional differences, $CD56^{bright}$ and $CD56^{dim}$ NK cells had similar fuel requirements. We concluded that human NK cells were relatively fuel resilient and continued to function even when both Glc and Gln were limited.

Human NK cells use Glc, Gln, fatty acid β-oxidation, or acetate

Because NK cells function in combined Glc and Gln deficiency, we hypothesized that NK cells use other energy sources to power cytokine production. Cells burn fatty acid (FA) via mitochondrial β-oxidation to produce ATP. To prevent β-oxidation, we treated cells with 3 μM ETO, a dose that inhibits the mitochondrial FA transporter, Cpt1a, and subsequent β-oxidation but which does have not known off-target effects (28, 29). We tested our hypothesis with a matrix of conditions including Glc or Gln deficiency, with or without 3 μM ETO to block FA β-oxidation during the entire 2-d culture (Fig. 5A). Under all fuel conditions, nearly 100% of $CD56^{bright}$ NK cells and the majority of $CD56^{dim}$ NK cells remained viable (Fig. 5B). We found that deficiencies of Glc, Gln, or β-oxidation individually failed to lower the percentage of IL-12/IL-18–stimulated human $CD56^{bright}$ and $CD56^{dim}$ NK cells that produce IFN-γ. Only triple Glc, Gln, and FA deficiency consistently reduced the number of IFN-γ–producing $CD56^{bright}$ and $CD56^{dim}$ NK cells (Fig. 5A).

Surprisingly, even in the absence of Glc and Gln and the presence of ETO to inhibit β-oxidation, nearly 50% of human $CD56^{bright}$ and $CD56^{dim}$ NK cells nonetheless produced some IFN-γ, although the amount of IFN-γ per cell was reduced to ~20% of control "full fuel" values (Supplemental Fig. 3D). Thus, nearly half of $CD56^{bright}$ and $CD56^{dim}$ NK cells produced some IFN-γ despite deficient Glc, Gln, and FA β-oxidation. This underscored the conclusion that human NK cells were fuel resilient.

Starting from pyruvate, cancer cells produce acetate and secrete it into the tumor microenvironment (30). After uptake into cells, acetate is converted into acetyl-CoA. Therefore, we explored whether NK cells used acetate. To limit other fuels, we stimulated NK cells with IL-12/IL-18 in the absence of Glc and Gln, with the addition of 3 μM ETO to inhibit FA β-oxidation. As before, the triple fuel deficiency diminished, but did not eliminate, human NK cell IFN-γ production (Fig. 5C). However, 20 mM acetate rescued $CD56^{dim}$ NK cell IFN-γ production (Fig. 5C) and viability (data not shown). These experiments indicated that human NK cells were relatively fuel resilient and used a variety of fuels, including Glc, Gln, FA, and acetate. These properties suggested that NK cells obtain various fuels in harsh environments, including infected tissues and tumors.

OxPhos is not necessary for CD8 T cell or NK cell cytokine production

Glc, Gln, and FA all can be burned as fuel by mitochondrial OxPhos. Furthermore, acetate is a product of OxPhos anaplerosis. This showed that OxPhos was sufficient for NK cell cytokine production. We investigated whether OxPhos was necessary for human CD8 or human NK cell IFN-γ production. Measured immediately ex vivo, CD8 T cells had higher mitochondrial content than did NK cells (Supplemental Fig. 4A). Among NK cells, immature $CD56^{bright}$ cells were slightly higher than mature $CD56^{dim}$ cells. To investigate the role of OxPhos in effector responses, we inhibited mitochondrial OxPhos using oligomycin, which has been used on lymphocytes at 0.015–2 μM (6, 11, 12). We found that oligomycin (0.1, 1, or 5 μM), which was present in the final 18 h of culture, did not significantly inhibit human $CD56^{bright}$ or $CD56^{dim}$ NK cell IFN-γ production (Supplemental Fig. 4B). Oligomycin at all three doses moderately reduced anti–CD3/CD28 bead–activated human CD8 T cell IFN-γ production from a very active donor but had little effect on CD8 T cells from other research subjects (Supplemental Fig. 4B and data not shown). Taken together, our data suggested that human CD8 T cells relied on glycolysis, but not OxPhos, as a major energy source and that NK cells used glycolysis or OxPhos.

Human CD8 T cell glycolysis requires Gln

We explored how Gln affected CD8 and NK cell metabolism. Anti–CD3/CD28 activated, IL-12/IL-18–stimulated human CD8 T cells were exposed to various Glc and Gln conditions, which were present from the start of the 2-d culture period and in Seahorse plates. Consistent with results shown above, Glc starvation greatly diminished ECAR by bead-activated human CD8 T cell (Fig. 6A). With no available Gln, bead-activated human CD8 T cells also greatly reduced ECAR, which indicated a marked reduction of glycolysis (Figs. 6A, 7A). Human CD8 T cell glycolysis dropped in the absence of Gln, despite abundant (11 mM) Glc. Thus, human CD8 T cells under bead activation conditions were unlike mouse CD4 and CD8 T cells deprived of Gln for 5 h, which moderately lowered

ECAR (9). As with mouse CD4 and CD8 T cells (9), Gln starvation greatly reduced human CD8 T cell OxPhos (OCR, Figs. 6B, 7B). As shown by oligomycin treatment (Supplemental Fig. 4B), OxPhos was not required for CD8 T cell effector functions. Human CD8 T cell ATP levels were also sensitive to Gln concentrations (Figs. 6C, 7C). Titration experiments showed that Gln concentrations ≤0.02 mM dropped human CD8 T cell ECAR, OCR, and ATP levels. In marked contrast, human NK cell ECAR and OCR were insensitive to Gln loss (Figs. 6A, 6B, 7A, 7B). Importantly, Gln starvation did not diminish NK cell ATP levels (Figs. 6C, 7C). As expected, Glc, Gln, and FA triple fuel deficiency reduced NK cell ATP level (Fig. 6C). It should be noted that human anti–CD3/CD28 bead–activated, IL-12/IL-18–stimulated CD8 T cells had much higher ECAR, OCR, and ATP under full fuel conditions, compared with IL-12/IL-18–stimulated NK cells (Figs. 6, 7). At 0.02 mM Gln, CD8 T cell and NK cells had similar ECAR, OCR, and ATP levels. Yet, at 0.02 mM Gln, CD8 T cells functioned poorly, but the percent responding NK cells did not decline (Fig. 4). Collectively, our data suggested that stimulated human CD8 T cell effector functions had much higher energy requirements than did human NK cells under the conditions tested.

Human CD8 T cells require Gln to suppress TXNIP and permit Glc uptake

In the presence of high Glc, some cells shut down glycolysis when Gln levels are low (31, 32). Mechanistically, TXNIP and ARRDC4 suppress Glc uptake, but are themselves regulated by Gln (31–33). Therefore, we measured TXNIP and ARRDC4 RNA levels in IL-12/IL-18–stimulated CD8 T cells and NK cells. TXNIP RNA was ~30- to 100-fold higher than ARRDC4 RNA in stimulated T and NK lymphocytes (data not shown), so we analyzed changes in TXNIP expression. In anti–CD3/CD28 bead–activated, IL-12/IL-18–stimulated human CD8 T cells, increasing Gln concentrations inversely correlated with TXNIP RNA in a dose-dependent fashion, rising nearly 6-fold in Gln starvation (Fig. 8A). In contrast, IL-12/IL-18–stimulated human NK cell TXNIP RNA did not change with Gln concentration (Fig. 8A). Results with anti–CD3/CD28 plate–activated human CD8 T cells were intermediate (Fig. 8A). We next examined whether Gln influences uptake of the fluorescent Glc analogue, 2-NBDG. Immediately ex vivo, human CD8 T cells and NK cells were very similar in 2-NBDG uptake (data not shown), which suggested similar Glc import. However, CD8 T cells and NK cells differed markedly after activation and stimulation in culture for 2 d without Gln. Anti–CD3/CD28 bead–activated human CD8 T cells stimulated with IL-12/IL-18 in the presence of 11 mM Glc and 2 mM Gln imported considerable Glc tracer (2-NBDG, Fig. 8B). However, low Gln significantly inhibited Glc uptake. Notably Glc uptake was highly significantly inhibited when the Gln level was ≤0.02 mM (Fig. 8B), a concentration that also greatly reduced IL-12/IL-18–stimulated IFN-γ and TNF-α expression (Fig. 4). For $CD56^{bright}$ and $CD56^{dim}$ NK cells and for plate-activated CD8 T cells, Gln starvation mildly affected Glc uptake (Fig. 8B). This paralleled the finding that Gln starvation did not diminish IL-12/IL-18–stimulated cytokine expression in those cells (Fig. 4). These results revealed a fundamental difference in Glc handling between human CD8 T cells and human NK cells. Because human CD8 T cell cytokine production requires glycolysis, TXNIP regulation of Glc uptake explained why strongly stimulated T cells required Gln. In contrast, human NK cells were fuel resilient. The TXNIP mechanism was not significantly activated in NK cells and was not suppressed by Gln.

DISCUSSION

Our work reveals three important findings. First, seemingly small differences in anti–CD3/CD28 activation cause profound differences in human CD8 T cell response to monokine stimulation under different fuel conditions. Second, strongly activated human CD8 T cells do not import Glc unless Gln is available. Third, human NK cells are much more fuel resilient than are human CD8 T cells. In this respect, they differ from Glc-addicted human CD8 effector T cells. To our knowledge, several aspects of this work have not been reported heretofore.

Investigators often activate T cells with a combination of anti-CD3 and anti-CD28 mAb to mimic aspects of peptide-MHC and CD80/CD86 costimulation. In one common method, anti-CD3 mAb is immobilized on plates and anti-CD28 mAb is soluble. In another common method, both mAbs are immobilized on beads. We refer to these two methods as plate and bead activation, which in our experiments with isolated human CD8 T cells usually was followed by IL-12/IL-18 stimulation. Anti–CD3/CD28 bead activation induce higher IL-12/IL-18–stimulated CD8 T cell cytokine and GzmB responses than do plate activation. Bead-activated CD8 T cells also have higher glycolysis and consume much higher O_2 than do plate-activated CD8 T cells. In the setting of Glc deprivation, bead-activated human CD8 T cells become hypofunctional, whereas plate-activated CD8 T cells die. To our knowledge, this phenomenon has not been previously reported, yet the two activation techniques seem to be treated as equivalent in the literature. The two anti–CD3/CD28 formats likely differ in strength or in quality. We are investigating possible mechanistic reasons for the differences.

Our most striking discovery concerns the mechanisms underlying CD8 T cell requirements for Gln. T lymphocytes rely on Gln for proliferation, cytokine production, and cell surface molecule expression (34, 35). Others showed that T cells use Gln as a fuel to maintain TCA intermediates and for ATP production (9, 36, 37), to provide the biosynthetic precursors of polyamines, nucleotides, and UDP *N*-acetylglucosamine (38, 39), and to maintain mTORC1 activity (40, 41). We describe a new role for Gln in strongly activated human CD8 effector T cells—Gln regulates Glc uptake. Despite their high responses, anti–CD3/CD28 bead–activated human CD8 T cells require Gln to express cytokines, to continue glycolysis, to consume O_2, and to maintain cellular ATP levels. Less vigorous plate-activated human CD8 T cells do not require Gln to produce cytokines or GzmB in response to IL-12/IL-18 stimulation. As noted above, human CD8 T cells activated under either condition require ample Glc for function or for cell viability.

We investigated why strongly activated human CD8 T cells require Gln for function and to maintain metabolism. The answer came from lessons learned in tumor cell metabolism. The MondoA-MLX transcription factor complex resides on the outer mitochondrial membrane (32). Upon binding to its physiologic ligand, Glc-6 phosphate, MondoA-MLX translocates to the nucleus and engages carbohydrate response elements on the promoters of Glc-responsive genes (32). MondoA-MLX highly upregulates TXNIP expression, which has pleiotropic functions, including repressing mTOR. Importantly for this discussion, TXNIP regulates glycolysis, acting as a feedback mechanism when glycolysis is high. TXNIP inhibits Glc uptake, at least in part, by binding to the GLUT1 Glc transporter and removing

it from the cell surface (32). TXNIP also may regulate other aspects of glycolysis. Interestingly, Gln inhibits Glc-6-phosphate-induced TXNIP expression at the level of the *TXNIP* promoter. Gln inhibits neither MondoA-MLX nuclear translocation nor *TXNIP* promoter binding. However, Gln does change the epigenetic landscape, which is reversed by inhibiting histone deacetylase (32).

We tested two key components of this pathway in human CD8 T cells. In the presence of ample (11 mM) Glc, we titrated Gln. When Gln concentration is lowered to ≤0.02 mM, TXNIP is induced and fluorescent 2-NBDG Glc tracer uptake is inhibited. The same Gln concentration prevents IL-12/IL-18–induced IFN-γ and TNF-α expression by anti–CD3/CD28 bead–activated human CD8 T cells. Gln concentration ≤0.02 mM decreases CD8 T cell glycolysis, OxPhos, and cellular ATP level. The TXNIP mechanism may explain prior findings that appear to contradict our own. Others have reported that 5 h of Gln starvation minimally reduced mouse CD4 and CD8 T cell ECAR (9). Because Gln causes epigenetic changes (31, 32), TXNIP protein levels might not change after only a 5-h Gln starvation. As noted above, we applied Gln starvation for the entire 2 d of culture. Further work will be required to test whether TXNIP regulates mTORC1 activation, nucleotide synthesis, polyamine synthesis or *O*-GlcNAcylation in human CD8 T cells. Conditions tested in these experiments may be relevant to sepsis, in which high Glc and low Gln are found (18–21).

Human NK cell metabolism and fuel requirements contrasts with those of human CD8 T cells. Most IL-12/IL-18–stimulated NK cells make IFN-γ and GzmB when glycolysis is blocked. This includes both immature $CD56^{bright}$ and mature $CD56^{dim}$ NK cells. CD8 T cell OCR decline when Glc concentration become very low. In contrast, NK cell OCR is maintained when glycolysis is inhibited, suggesting that human NK cells maintain metabolic function in the absence of Glc. This conclusion was supported by measuring ATP levels. CD8 T cell ATP level declines in concert with glycolysis. In contrast, human NK cells maintain nearly constant ATP concentrations, even as glycolysis is prohibited. These data suggest that human NK cells are relatively fuel resilient. Furthermore, NK cells function well when deprived of Gln. Indeed, the absence of both fuels does not eliminate NK cell IFN-γ production, O_2 consumption, or cellular ATP levels. Remarkably, even when FA β-oxidation is inhibited by ETO, Glc, and Gln starvation lowers, but does not abrogate, IL-12/IL-18–stimulated human NK cell IFN-γ synthesis. As expected, Glc starvation inhibits glycolysis and the combined absence of available Glc, Gln, and FA β-oxidation reduces NK cell O_2 consumption and ATP level. Remarkably, acetate rescues NK cell function.

Our work can be compared with published studies. Cooper's group found that mouse NK cells stimulated with IL-12/IL-18 made similar amounts of IFN-γ, even after 4–6 h incubation with oligomycin and 2-deoxy-D-Glc (2DG), in the absence of Gln (12). Our findings are largely consistent with the conclusions suggested by these experiments, namely that NK cells are fuel resilient. Other work suggested that mouse NK cells required glycolysis for cytokine production and other functions. For example, Donnelly et al. (11) showed that 2DG and substitution of Gal for Glc had moderate effects on IFN-γ production. Loftus et al. (42) reported that 20-h Gln starvation decreased NK cell IFN-γ production. It is not clear whether these variances from our findings were due to species differences, stimulation differences, or the fact that the mouse NK cells were stimulated in the setting

of unseparated splenocytes. The mouse NK cells in these studies underwent a long culture period in the presence of splenic T cells, B cells, and myeloid cells, which may have influenced NK cell behavior. In the context of human PBMC, Keating et al. (13) reported that oligomycin decreased human NK cell IFN-γ synthesis in response to 18-h IL-12/IL-15 stimulation. In contrast, we found that oligomycin did not inhibit IFN-γ responses by IL-12/IL-18–stimulated enriched NK cells. It may be significant that Keating et al. (13) studied human NK cells in the context of unseparated PBMC because the presence of T cells, B cells, monocytes and other PBMC may have influenced NK cells.

Given the minimal effect that Gln starvation has on human NK cell function, metabolism and ATP levels, it is not surprising that Gln deprivation does not alter TXNIP expression and only mildly affects Glc uptake. Thus, NK cell glycolysis does not appear to be regulated by the MondoA-MLX and TXNIP pathways, at least under the conditions tested in this study. TXNIP RNA is expressed both by developing and by mature mouse NK cells, and the *TXNIP* gene is required for NK cell CD122 expression and for mouse NK cell development (43). These findings suggest that an inability to express TXNIP in NK cells does not account for differential Glc handing by CD8 T cell and NK cells. Also, “weak” plate–activated CD8 T cells were minimally affected by ≤0.02 mM Gln in ample Glc. Low Gln did not significantly diminish Glc uptake and only moderately induced TXNIP expression by anti–CD3/CD28 plate–activated, IL-12/IL-18–stimulated human CD8 T cells. We are investigating why MondoA-MLX-TXNIP regulates human CD8 T cells following “strong” anti–CD3/CD28 bead –activated, but not following “weak” plate-activated, CD8 T cell stimulation or NK cell stimulation.

Our human CD8 T cell experiments confirm and extend the work of others. As found with mouse and human T cells, either low Glc or 2DG inhibited cytokine production in response to anti–CD3/CD28, with or without additional IL-2 (6, 7, 9, 10, 44–46). Notably, responses were optimal in 25–35 mM Glc and were somewhat blunted by 0.35 or even 10 mM Glc (9, 46). Confirming these general findings, we found that human CD8 T cells require glycolysis for optimal cytokine and GzmB responses to anti–CD3/CD28 activation and IL-12/IL-18 stimulation. We inhibited glycolysis using low Glc and substitution of Glc with Gal. We purposely avoided 2DG, which has well-documented toxic effects beyond inhibiting hexokinase (47, 48). T cell effector responses, especially IFN-γ production, are well-known to rely on glycolysis, and two mechanisms have been advanced to explain effector T cell Glc addiction. The translation inhibition hypothesis states that GAPDH, when not actively engaged in glycolysis, binds the IFN-γ mRNA 3′UTR and prevent its translation (6). The epigenetic hypothesis states that steady-state acetyl-CoA levels fall when glycolysis is low (7). This leads to a reduction in acetylated histones at the *IFNG* locus, and thus lowering transcription (7). We found that Glc starvation lowers human CD8 T cell IFN-γ and GzmB mRNA, which is not easily explained by the translation inhibition hypothesis but appears consistent with the epigenetic hypothesis. However, TNF-α RNA does not change markedly with mildly depressed Glc concentration, and TNF-α expression may be subject to GAPDH-mediated translation suppression, as reported in macrophages (49).

CD8 T cells and NK cells are the two major cytotoxic lymphocytes. They kill aberrant cells and secrete IFN-γ and TNF-α. As such, they defend against cancers, viruses, and other intracellular parasites. These settings are often low in Glc and Gln. Human serum Glc ranges from 3.9 to 7.8 mM. Blood Gln is ~0.478–0.550 mM but is considerably lower in severe infection (20, 27). In experimental tumors, Glc has been estimated to range from undetectable to 1.3 mM (8, 15), and Gln from 0.1 to 0.7 mM (16, 17). In human pancreatic carcinomas, Gln had the lowest relative concentration of all the amino acids (16). In this study, we show that human effector CD8 T cells require both Glc and Gln. Furthermore, we have elucidated a novel mechanism by which Gln controls Glc usage in human CD8 T cells. This and other knowledge to be gained may help us to program powerful human CD8 T cells to function in infected sites and in tumors. This is especially relevant to chimeric Ag receptor T cells, which have shown remarkable success with leukemias and lymphomas but have not been effective in solid malignancies (50).

Compared with CD8 T cells, human NK cells are fuel resilient and use Glc, Gln, FA, and even acetate to fuel effector functions. Therefore, NK cells may function in infected sites or tumor environments in which effector CD8 T cells do not function (8, 14–17). NK cells help control several cancers (51–55) and prevent metastases (56, 57). Cancer stem cells are especially susceptible to NK cell attack (58, 59). In some established tumors, NK cells localize at the tumor periphery (60). This is where cancer stem cells with the highest metastatic potential are found in some cancers (61). However, NK cells often do not infiltrate the tumor interior (60). Tumor infiltration is governed by a combination of chemokines and cellular addressin (62). If they can be engineered to respond to tumor-infiltrating signals, fuel-resilient NK cells may be even more effective cancer-fighting cells.

Supplementary Material

Refer to Web version on PubMed Central for supplementary material.

ACKNOWLEDGMENTS

We thank the human subjects who kindly donated blood in these experiments; C. Darrell Jennings, Barbara Nikolajczyk, Ramon Sun, Jessica K. A. Macedo, E. Charles Snow, and Suzanne Segerstrom for helpful discussions; and Michael Alstott and Tomoko Sengoku for help with Seahorse experiments.

This work was supported by the National Center for Research Resources and the National Center for Advancing Translational Sciences through National Institutes of Health Grant UL1TR000117, the University of Kentucky College of Medicine, and the University of Kentucky Department of Pathology and Laboratory Medicine. T.R. was supported by the University of Kentucky/Appalachian Career Training in Oncology Program (under National Institutes of Health/National Cancer Institute Grant NCI R25CA221765). The University of Kentucky Redox Metabolism Shared Resource Facility is supported by National Cancer Institute/Cancer Center Support Grant P30 CA177558. The University of Kentucky Flow Cytometry facility is supported in part by a National Cancer Institute/Cancer Center Support Grant (P30 CA177558) to the University of Kentucky Markey Cancer Center.

Abbreviations used in this article:

2DG	2-deoxy-D-Glc
ECAR	extracellular acidification rate
ETO	etomoxir

FA	fatty acid
Gal	galactose
Glc	glucose
Gln	glutamine
MFI	median fluorescence intensity
2-NBDG	2-[*N*-(7-nitrobenz-2-oxa-1,3-diazol-4-yl)amino]-2-deoxy-D-glucose
OCR	oxygen consumption rate
TXNIP	thioredoxin-interacting protein

REFERENCES

1. Trinchieri G 1989. Biology of natural killer cells. Adv. Immunol. 47: 187–376. [PubMed: 2683611]
2. Tian Z, Gershwin ME, and Zhang C 2012. Regulatory NK cells in autoimmune disease. J. Autoimmun. 39: 206–215. [PubMed: 22704425]
3. Waggoner SN, Cornberg M, Selin LK, and Welsh RM 2011. Natural killer cells act as rheostats modulating antiviral T cells. Nature 481: 394–398. [PubMed: 22101430]
4. Akane K, Kojima S, Mak TW, Shiku H, and Suzuki H 2016. CD8+CD122+CD49dlow regulatory T cells maintain T-cell homeostasis by killing activated T cells via Fas/FasL-mediated cytotoxicity. Proc. Natl. Acad. Sci. USA 113: 2460–2465. [PubMed: 26869716]
5. Zhang N, and Bevan MJ 2011. CD8(+) T cells: foot soldiers of the immune system. Immunity 35: 161–168. [PubMed: 21867926]
6. Chang CH, Curtis JD, Maggi LB Jr., Faubert B, Villarino AV, O'Sullivan D, Huang SC, van der Windt GJ, Blagih J, Qiu J, et al. 2013. Posttranscriptional control of T cell effector function by aerobic glycolysis. Cell 153: 1239–1251. [PubMed: 23746840]
7. Peng M, Yin N, Chhangawala S, Xu K, Leslie CS, and Li MO 2016. Aerobic glycolysis promotes T helper 1 cell differentiation through an epigenetic mechanism. Science 354: 481–484. [PubMed: 27708054]
8. Ho PC, Bihuniak JD, Macintyre AN, Staron M, Liu X, Amezquita R, Tsui YC, Cui G, Micevic G, Perales JC, et al. 2015. Phosphoenolpyruvate is a metabolic checkpoint of anti-tumor T cell responses. Cell 162: 1217–1228. [PubMed: 26321681]
9. Blagih J, Coulombe F, Vincent EE, Dupuy F, Galicia-Vázquez G, Yurchenko E, Raissi TC, van der Windt GJ, Viollet B, Pearce EL, et al. 2015. The energy sensor AMPK regulates T cell metabolic adaptation and effector responses in vivo. Immunity 42: 41–54. [PubMed: 25607458]
10. Cham CM, and Gajewski TF 2005. Glucose availability regulates IFN-gamma production and p70S6 kinase activation in CD8+ effector T cells. J. Immunol. 174: 4670–4677. [PubMed: 15814691]
11. Donnelly RP, Loftus RM, Keating SE, Liou KT, Biron CA, Gardiner CM, and Finlay DK 2014. mTORC1-dependent metabolic reprogramming is a prerequisite for NK cell effector function. J. Immunol. 193: 4477–4484. [PubMed: 25261477]
12. Keppel MP, Saucier N, Mah AY, Vogel TP, and Cooper MA 2015. Activation-specific metabolic requirements for NK Cell IFN-γ production. J. Immunol. 194: 1954–1962. [PubMed: 25595780]
13. Keating SE, Zaiatz-Bittencourt V, Loftus RM, Keane C, Brennan K, Finlay DK, and Gardiner CM 2016. Metabolic reprogramming supports IFN-γ production by $CD56^{bright}$ NK cells. J. Immunol. 196: 2552–2560. [PubMed: 26873994]
14. Baud MO, Vitt JR, Robbins NM, Wabl R, Wilson MR, Chow FC, Gelfand JM, Josephson SA, and Miller S 2017. Pleocytosis is not fully responsible for low CSF glucose in meningitis. Neurol. Neuroimmunol. Neuroinflamm. 5: e425. [PubMed: 29296633]

15. Gullino PM, Clark SH, and Grantham FH 1964. The interstitial fluid of solid tumors. Cancer Res. 24: 780–794. [PubMed: 14190544]
16. Kamphorst JJ, Nofal M, Commisso C, Hackett SR, Lu W, Grabocka E, Vander Heiden MG, Miller G, Drebin JA, BarSagi D, et al. 2015. Human pancreatic cancer tumors are nutrient poor and tumor cells actively scavenge extracellular protein. Cancer Res. 75: 544–553. [PubMed: 25644265]
17. Pan M, Reid MA, Lowman XH, Kulkarni RP, Tran TQ, Liu X, Yang Y, Hernandez-Davies JE, Rosales KK, Li H, et al. 2016. Regional glutamine deficiency in tumours promotes dedifferentiation through inhibition of histone demethylation. Nat. Cell Biol. 18: 1090–1101. [PubMed: 27617932]
18. Wernly B, Lichtenauer M, Hoppe UC, and Jung C 2016. Hyperglycemia in septic patients: an essential stress survival response in all, a robust marker for risk stratification in some, to be messed with in none. J. Thorac. Dis. 8: E621–E624. [PubMed: 27501420]
19. Marik PE, and Bellomo R 2013. Stress hyperglycemia: an essential survival response! Crit. Care 17: 305. [PubMed: 23470218]
20. Kao C, Hsu J, Bandi V, and Jahoor F 2013. Alterations in glutamine metabolism and its conversion to citrulline in sepsis. Am. J. Physiol. Endocrinol. Metab. 304: E1359–E1364. [PubMed: 23612995]
21. Karinch AM, Pan M, Lin CM, Strange R, and Souba WW 2001. Glutamine metabolism in sepsis and infection. J. Nutr. 131(Suppl.): 2535S–2538S, discussion 2550S–2551S. [PubMed: 11533308]
22. Schenkel JM, and Masopust D 2014. Tissue-resident memory T cells. Immunity 41: 886–897. [PubMed: 25526304]
23. Horton BL, Williams JB, Cabanov A, Spranger S, and Gajewski TF 2018. Intratumoral $CD8^+$ T-cell apoptosis is a major component of T-cell dysfunction and impedes antitumor immunity. Cancer Immunol. Res. 6: 14–24. [PubMed: 29097422]
24. Renner K, Geiselhöringer AL, Fante M, Bruss C, Färber S, Schönhammer G, Peter K, Singer K, Andreesen R, Hoffmann P, et al. 2015. Metabolic plasticity of human T cells: preserved cytokine production under glucose deprivation or mitochondrial restriction, but 2-deoxy-glucose affects effector functions. Eur. J. Immunol. 45: 2504–2516. [PubMed: 26114249]
25. Marçais A, Cherfils-Vicini J, Viant C, Degouve S, Viel S, Fenis A, Rabilloud J, Mayol K, Tavares A, Bienvenu J, et al. 2014. The metabolic checkpoint kinase mTOR is essential for IL-15 signaling during the development and activation of NK cells. Nat. Immunol. 15: 749–757. [PubMed: 24973821]
26. Harty JT, Tvinnereim AR, and White DW 2000. $CD8^+$ T cell effector mechanisms in resistance to infection. Annu. Rev. Immunol. 18: 275–308. [PubMed: 10837060]
27. Levine R 1986. Monosaccharides in health and disease. Annu. Rev. Nutr. 6: 211–224. [PubMed: 3524617]
28. O'Connor RS, Guo L, Ghassemi S, Snyder NW, Worth AJ, Weng L, Kam Y, Philipson B, Trefely S, Nunez-Cruz S, et al. 2018. The CPT1a inhibitor, etomoxir induces severe oxidative stress at commonly used concentrations. Sci. Rep. 8: 6289. [PubMed: 29674640]
29. Raud B, Roy DG, Divakaruni AS, Tarasenko TN, Franke R, Ma EH, Samborska B, Hsieh WY, Wong AH, Stuve P, et al. 2018. Etomoxir actions on regulatory and memory T cells are independent of Cpt1a-mediated fatty acid oxidation. Cell Metab. 28: 504–515.e7. [PubMed: 30043753]
30. Liu X, Cooper DE, Cluntun AA, Warmoes MO, Zhao S, Reid MA, Liu J, Lund PJ, Lopes M, Garcia BA, et al. 2018. Acetate production from glucose and coupling to mitochondrial metabolism in mammals. Cell 175: 502–513.e13. [PubMed: 30245009]
31. Kaadige MR, Looper RE, Kamalanaadhan S, and Ayer DE 2009. Glutamine-dependent anapleurosis dictates glucose uptake and cell growth by regulating MondoA transcriptional activity. Proc. Natl. Acad. Sci. USA 106: 14878–14883. [PubMed: 19706488]
32. O'Shea JM, and Ayer DE 2013. Coordination of nutrient availability and utilization by MAX- and MLX-centered transcription networks. Cold Spring Harb. Perspect. Med. 3: a014258. [PubMed: 24003245]

33. Parikh H, Carlsson E, Chutkow WA, Johansson LE, Storgaard H, Poulsen P, Saxena R, Ladd C, Schulze PC, Mazzini MJ, et al. 2007. TXNIP regulates peripheral glucose metabolism in humans. PLoS Med. 4: e158. [PubMed: 17472435]
34. Hörig H, Spagnoli GC, Filgueira L, Babst R, Gallati H, Harder F, Juretic A, and Heberer M 1993. Exogenous glutamine requirement is confined to late events of T cell activation. J. Cell. Biochem. 53: 343–351. [PubMed: 7905486]
35. Carr EL, Kelman A, Wu GS, Gopaul R, Senkevitch E, Aghvanyan A, Turay AM, and Frauwirth KA 2010. Glutamine uptake and metabolism are coordinately regulated by ERK/MAPK during T lymphocyte activation. J. Immunol. 185: 1037–1044. [PubMed: 20554958]
36. Guppy M, Greiner E, and Brand K 1993. The role of the Crabtree effect and an endogenous fuel in the energy metabolism of resting and proliferating thymocytes. Eur. J. Biochem. 212: 95–99. [PubMed: 8444168]
37. Cao Y, Rathmell JC, and Macintyre AN 2014. Metabolic reprogramming towards aerobic glycolysis correlates with greater proliferative ability and resistance to metabolic inhibition in CD8 versus CD4 T cells. PLoS One 9: e104104. [PubMed: 25090630]
38. Wang R, Dillon CP, Shi LZ, Milasta S, Carter R, Finkelstein D, McCormick LL, Fitzgerald P, Chi H, Munger J, and Green DR 2011. The transcription factor Myc controls metabolic reprogramming upon T lymphocyte activation. Immunity 35: 871–882. [PubMed: 22195744]
39. Swamy M, Pathak S, Grzes KM, Damerow S, Sinclair LV, van Aalten DM, and Cantrell DA 2016. Glucose and glutamine fuel protein O-GlcNAcylation to control T cell self-renewal and malignancy. Nat. Immunol. 17: 712–720. [PubMed: 27111141]
40. Jewell JL, Kim YC, Russell RC, Yu FX, Park HW, Plouffe SW, Tagliabracci VS, and Guan KL 2015. Metabolism. Differential regulation of mTORC1 by leucine and glutamine. Science 347: 194–198. [PubMed: 25567907]
41. Nakaya M, Xiao Y, Zhou X, Chang JH, Chang M, Cheng X, Blonska M, Lin X, and Sun SC 2014. Inflammatory T cell responses rely on amino acid transporter ASCT2 facilitation of glutamine uptake and mTORC1 kinase activation. Immunity 40: 692–705. [PubMed: 24792914]
42. Loftus RM, Assmann N, Kedia-Mehta N, O'Brien KL, Garcia A, Gillespie C, Hukelmann JL, Oefner PJ, Lamond AI, Gardiner CM, et al. 2018. Amino acid-dependent cMyc expression is essential for NK cell metabolic and functional responses in mice. Nat. Commun. 9: 2341. [PubMed: 29904050]
43. Lee KN, Kang HS, Jeon JH, Kim EM, Yoon SR, Song H, Lyu CY, Piao ZH, Kim SU, Han YH, et al. 2005. VDUP1 is required for the development of natural killer cells. Immunity 22: 195–208. [PubMed: 15723808]
44. Gubser PM, Bantug GR, Razik L, Fischer M, Dimeloe S, Hoenger G, Durovic B, Jauch A, and Hess C 2013. Rapid effector function of memory CD8+ T cells requires an immediate-early glycolytic switch. Nat. Immunol. 14: 1064–1072. [PubMed: 23955661]
45. Macintyre AN, Gerriets VA, Nichols AG, Michalek RD, Rudolph MC, Deoliveira D, Anderson SM, Abel ED, Chen BJ, Hale LP, and Rathmell JC 2014. The glucose transporter Glut1 is selectively essential for CD4 T cell activation and effector function. Cell Metab. 20: 61–72. [PubMed: 24930970]
46. Ecker C, Guo L, Voicu S, Gil-de-Gómez L, Medvec A, Cortina L, Pajda J, Andolina M, Torres-Castillo M, Donato JL, et al. 2018. Differential reliance on lipid metabolism as a salvage pathway underlies functional differences of T cell subsets in poor nutrient environments. Cell Rep. 23: 741–755. [PubMed: 29669281]
47. Kurtoglu M, Gao N, Shang J, Maher JC, Lehrman MA, Wangpaichitr M, Savaraj N, Lane AN, and Lampidis TJ 2007. Under normoxia, 2-deoxy-D-glucose elicits cell death in select tumor types not by inhibition of glycolysis but by interfering with N-linked glycosylation. Mol. Cancer Ther. 6: 3049–3058. [PubMed: 18025288]
48. MacFarlane M, Robinson GL, and Cain K 2012. Glucose–a sweet way to die: metabolic switching modulates tumor cell death. Cell Cycle 11: 3919–3925. [PubMed: 22983094]
49. Millet P, Vachharajani V, McPhail L, Yoza B, and McCall CE 2016. GAPDH binding to TNF-α mRNA contributes to posttranscriptional repression in monocytes: a novel mechanism of

communication between inflammation and metabolism. J. Immunol. 196: 2541–2551. [PubMed: 26843329]

50. Kakarla S, and Gottschalk S 2014. CAR T cells for solid tumors: armed and ready to go? Cancer J. 20: 151–155. [PubMed: 24667962]
51. Morvan MG, and Lanier LL 2016. NK cells and cancer: you can teach innate cells new tricks. Nat. Rev. Cancer 16: 7–19. [PubMed: 26694935]
52. Ferreira-Teixeira M, Paiva-Oliveira D, Parada B, Alves V, Sousa V, Chijioke O, Münz C, Reis F, Rodrigues-Santos P, and Gomes C 2016. Natural killer cell-based adoptive immunotherapy eradicates and drives differentiation of chemoresistant bladder cancer stem-like cells. BMC Med. 14: 163. [PubMed: 27769244]
53. Rusakiewicz S, Semeraro M, Sarabi M, Desbois M, Locher C, Mendez R, Vimond N, Concha A, Garrido F, Isambert N, et al. 2013. Immune infiltrates are prognostic factors in localized gastrointestinal stromal tumors. Cancer Res. 73: 3499–3510. [PubMed: 23592754]
54. Miller JS, Soignier Y, Panoskaltsis-Mortari A, McNearney SA, Yun GH, Fautsch SK, McKenna D, Le C, Defor TE, Burns LJ, et al. 2005. Successful adoptive transfer and in vivo expansion of human haploidentical NK cells in patients with cancer. Blood 105: 3051–3057. [PubMed: 15632206]
55. Coca S, Perez-Piqueras J, Martinez D, Colmenarejo A, Saez MA, Vallejo C, Martos JA, and Moreno M 1997. The prognostic significance of intratumoral natural killer cells in patients with colorectal carcinoma. Cancer 79: 2320–2328. [PubMed: 9191519]
56. Chockley PJ, Chen J, Chen G, Beer DG, Standiford TJ, and Keshamouni VG 2018. Epithelial-mesenchymal transition leads to NK cell-mediated metastasis-specific immunosurveillance in lung cancer. J. Clin. Invest. 128: 1384–1396. [PubMed: 29324443]
57. Hanna RN, Cekic C, Sag D, Tacke R, Thomas GD, Nowyhed H, Herrley E, Rasquinha N, McArdle S, Wu R, et al. 2015. Patrolling monocytes control tumor metastasis to the lung. Science 350: 985–990. [PubMed: 26494174]
58. Tallerico R, Todaro M, Di Franco S, Maccalli C, Garofalo C, Sottile R, Palmieri C, Tirinato L, Pangigadde PN, La Rocca R, et al. 2013. Human NK cells selective targeting of colon cancer-initiating cells: a role for natural cytotoxicity receptors and MHC class I molecules. J. Immunol. 190: 2381–2390. [PubMed: 23345327]
59. Ames E, Canter RJ, Grossenbacher SK, Mac S, Chen M, Smith RC, Hagino T, Perez-Cunningham J, Sckisel GD, Urayama S, et al. 2015. NK cells preferentially target tumor cells with a cancer stem cell phenotype. J. Immunol. 195: 4010–4019. [PubMed: 26363055]
60. Schneider T, Kimpfler S, Warth A, Schnabel PA, Dienemann H, Schadendorf D, Hoffmann H, and Umansky V 2011. Foxp3(+) regulatory T cells and natural killer cells distinctly infiltrate primary tumors and draining lymph nodes in pulmonary adenocarcinoma. J. Thorac. Oncol. 6: 432–438. [PubMed: 21258248]
61. Hermann PC, Huber SL, Herrler T, Aicher A, Ellwart JW, Guba M, Bruns CJ, and Heeschen C 2007. Distinct populations of cancer stem cells determine tumor growth and metastatic activity in human pancreatic cancer. Cell Stem Cell 1: 313–323. [PubMed: 18371365]
62. Lanitis E, Dangaj D, Irving M, and Coukos G 2017. Mechanisms regulating T-cell infiltration and activity in solid tumors. Ann. Oncol. 28(suppl_12): xii18–xii32. [PubMed: 29045511]

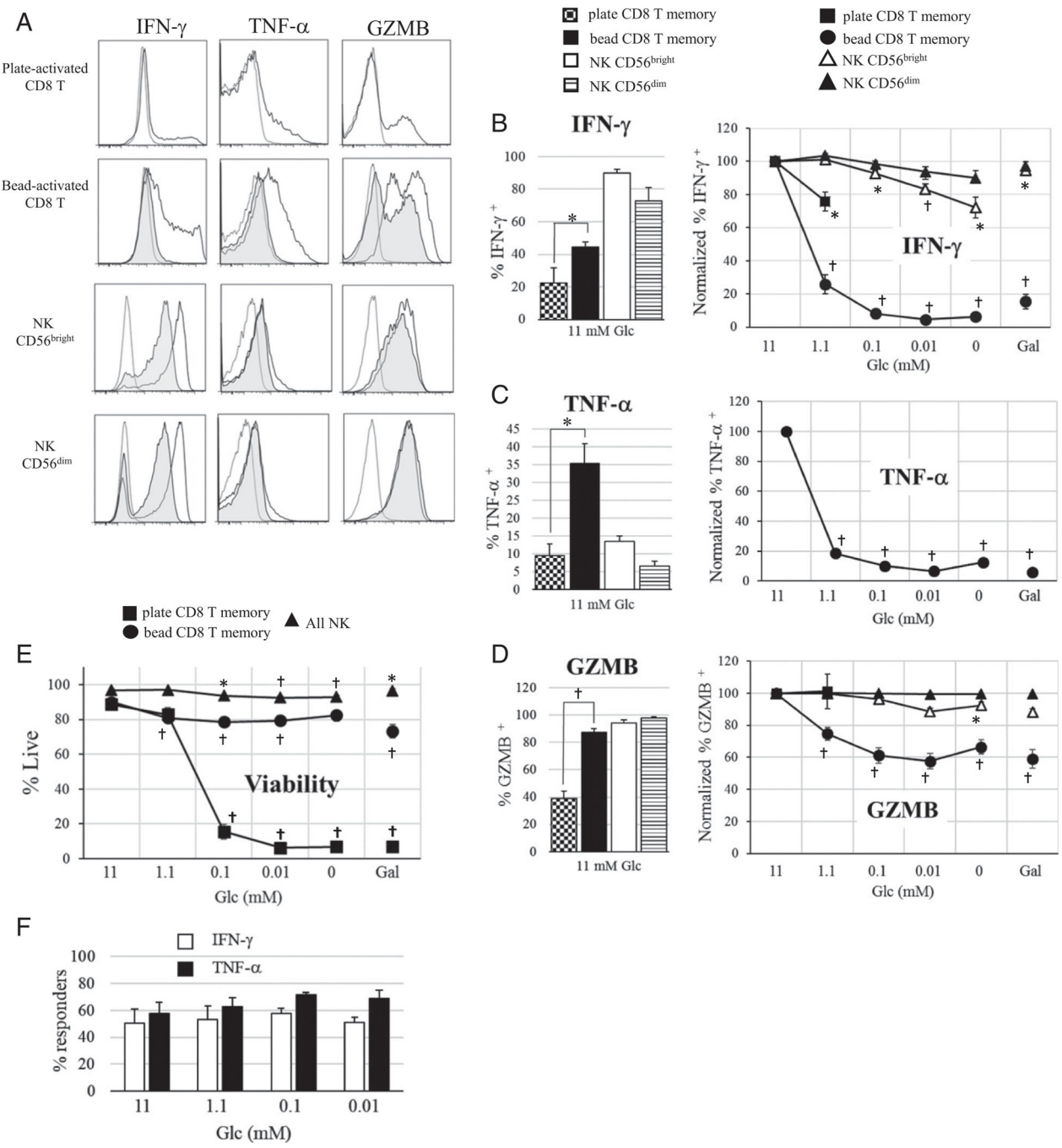

FIGURE 1. Human CD8 T cells require glycolysis for viability or for cytokine and GzmB expression, but NK cells express IFN-γ and GzmB when glycolysis is low.

Purified human CD8 T cells were anti–CD3/CD28 plate–activated (plate) or bead–activated (bead) for 2 d. Purified human NK cells were cultured in media for 2 d. IL-12/IL-18 was added to all groups in the final 24 h. Media contained the indicated Glc concentration, or Gal was substituted for Glc from the start of the 2-d culture. (**A**) Flow cytometry histograms are shown for a representative research subject. Dotted line is isotype mAb control, open histogram is 11 mM Glc, filled histogram is 11 mM Gal in place of Glc.

Gal results are not shown for plate-activated CD8 T cells because of the massive cell death. (**B–D**) Histogram plots represent average responses at 11 mM Glc. In the histogram plots, significant differences are indicated between plate-activated and bead-activated CD8 T cells, both at 11 mM Glc. Dot and line plots indicate changes in cytokine or GzmB expression normalized to 11 mM Glc. (B and D) IFN-γ and GzmB expression is not shown for plate-activated CD8 T cells at <1 mM Glc or in Gal, because of cell death. (C) Only bead-activated CD8 T cell results are shown with decreasing Glc concentrations or with Gal because of marginal TNF-α production by plate-activated CD8 T cell and NK cells, even in 11 mM Glc. (**E**) Cell viability, measured as described in Materials and Methods. (**F**) Purified CD8 T cells were bead activated for 2 d and stimulated with PMA and A23187 calcium ionophore during the final 5 h culture, as described in Materials and Methods. Glc concentrations at culture initiation are indicated on the x-axis. Cells from four to five research subjects (B–E) or three research subjects (F) were studied. In the dot and line plots, statistical difference are noted within the same cell type and activation technique, comparing 11 mM Glc and other fuel conditions. $^{*}p < 0.05$, $^{\dagger}p < 0.01$.

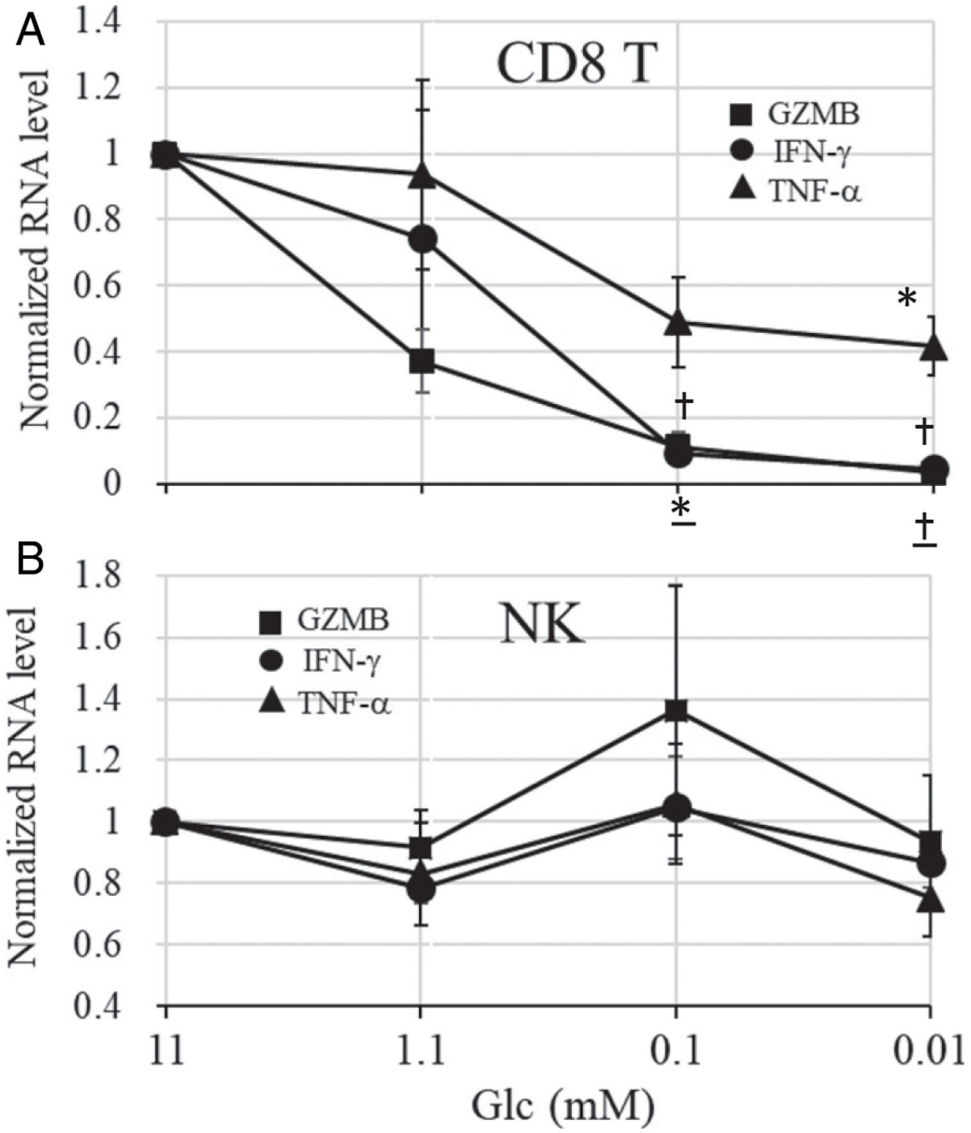

FIGURE 2. Differential effect of low Glc on CD8 T cell TNF-α mRNA level compared with GzmB and IFN-γ mRNA levels.

Bead-activated purified CD8 T cells (**A**) and purified NK cells (**B**) from four and three research subjects were IL-12/IL-18 stimulated as described in Materials and Methods. The Glc concentrations at culture initiation are indicated. Significant CD8 T cell differences from the 11 mM Glc condition are indicated under the x-axis for GzmB. $^{*}p < 0.05$, $^{\dagger}p < 0.01$, compared with 11 mM condition.

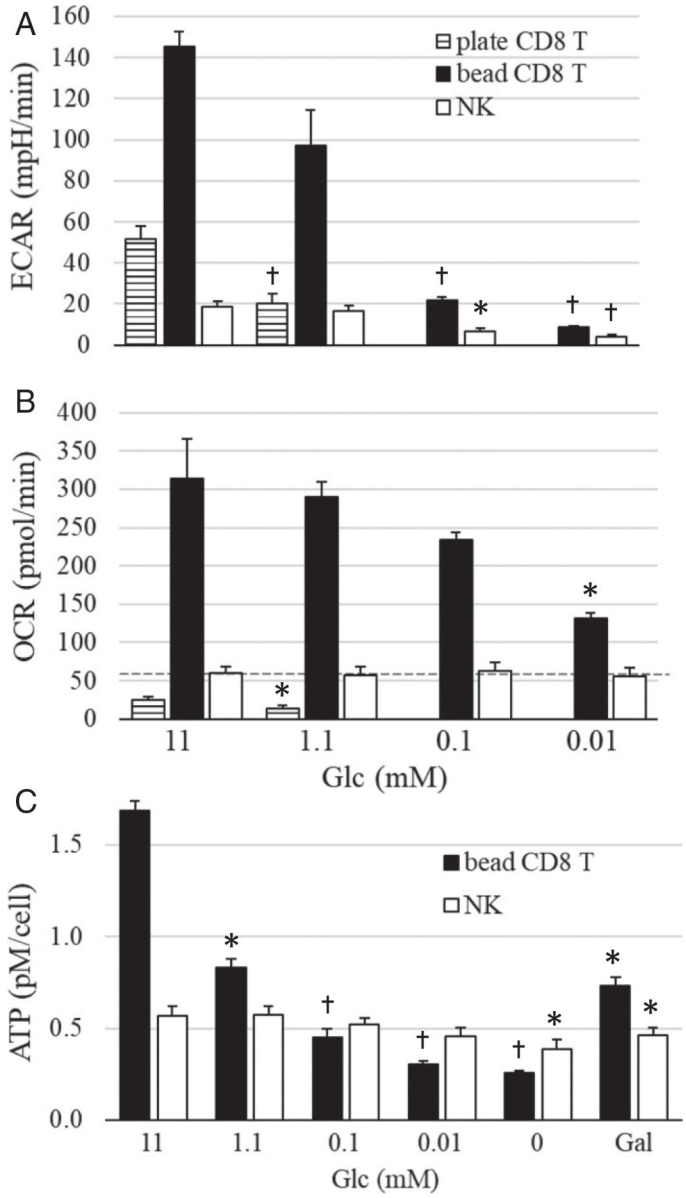

FIGURE 3. CD8 T cells require Glc for ECAR, OCR, and ATP maintenance, but Glc concentration does not affect NK cell OCR and has little effect on NK cell ATP level.

Purified cells were activated and stimulated, and ECAR (**A**), OCR (**B**), and ATP, per plated cell (**C**), were measured as described above. For ease of comparison, a dashed line in (B) denotes NK cell OCR in 11 mM Glc. The Glc concentrations at culture initiation and in the Seahorse instrument are indicated. For this figure, comparison data did not have equivalent variance and these data were log transformed prior to Student *t* test. $*p < 0.05$, $^{\dagger}p < 0.01$, compared with 11 mM condition within the same cell type and activation technique, generated from four subjects (A and B) and three subjects (C).

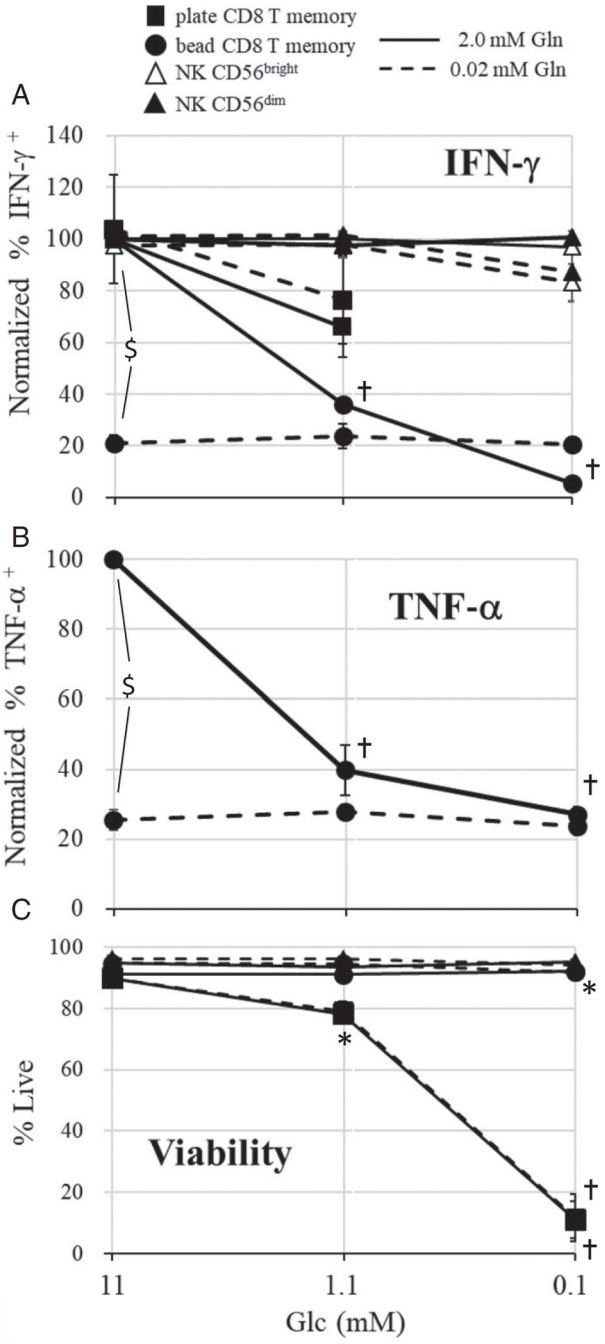

FIGURE 4. CD8 T cell cytokine production requires both Glc and Gln, but NK cells are relatively fuel resilient.

Purified cells were activated and stimulated, and IFN-γ expression (**A**), TNF-α expression (**B**), and cell viability (**C**) were measured as described above in cells from four subjects. The Glc concentrations at culture initiation are indicated on the x-axis. Solid lines denote 2 mM Gln, dashed lines denote 0.02 mM Gln at culture initiation. In (A), the results are normalized from 21.5% (plate-activated CD8), 46.7% (bead-activated CD8), 95.7% (CD56^{bright} NK), and 81.9% (CD56^{dim} NK) IFN-γ–producing cells. In (B), the results are normalized from

38.2% TNF-α–producing bead–activated CD8 T cells. Highly significant differences ($^{\$}p < 0.01$) between 2 mM and 0.02 mM Gln are indicated for bead-activated CD8 T cells at 11 mM Glc. $^{*}p < 0.05$, $^{\dagger}p < 0.01$, compared with 11 mM Glc condition within the same cell type and activation technique.

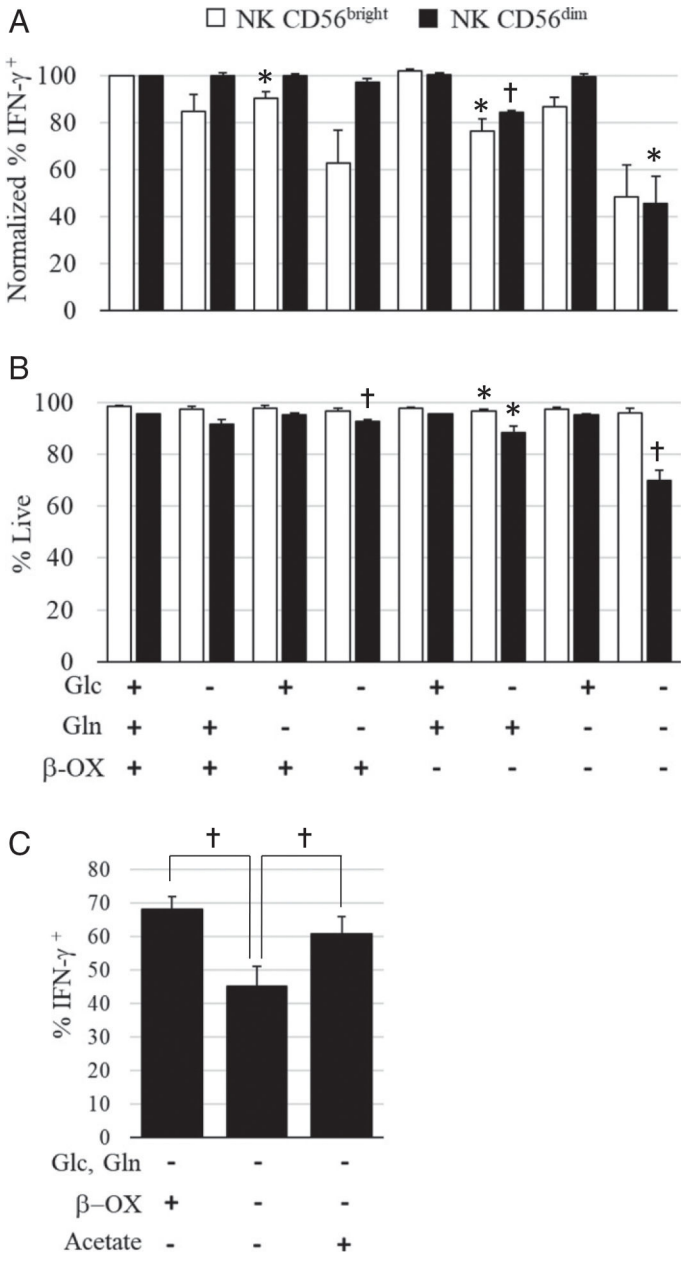

FIGURE 5. NK cells are relatively fuel resilient.

Purified human NK cells were activated and stimulated, and IFN-γ expression (**A** and **C**) and cell viability (**B**) were measured as described above in cells from four subjects. Results are normalized (A) from 11 mM Glc responses of 90.7% and 80.4% for $CD56^{bright}$ and $CD56^{dim}$ NK cells, respectively. Also shown are percentage live NK cells (B) and percentage IFN-γ–producing $CD56^{dim}$ NK cells (C). At initiation, cultures contained 0 or 11 mM Glc, 0 or 2 mM Gln. FA β-oxidation (β-oX) was allowed to proceed (+) or was blocked with 3 μM ETO (−). Some cultures were supplemented with 20 mM acetate (Acetate +). $^{*}p < 0.05$; $^{\dagger}p < 0.01$, compared with the 11 mM Glc/2 mM Gln/no ETO condition or as indicated.

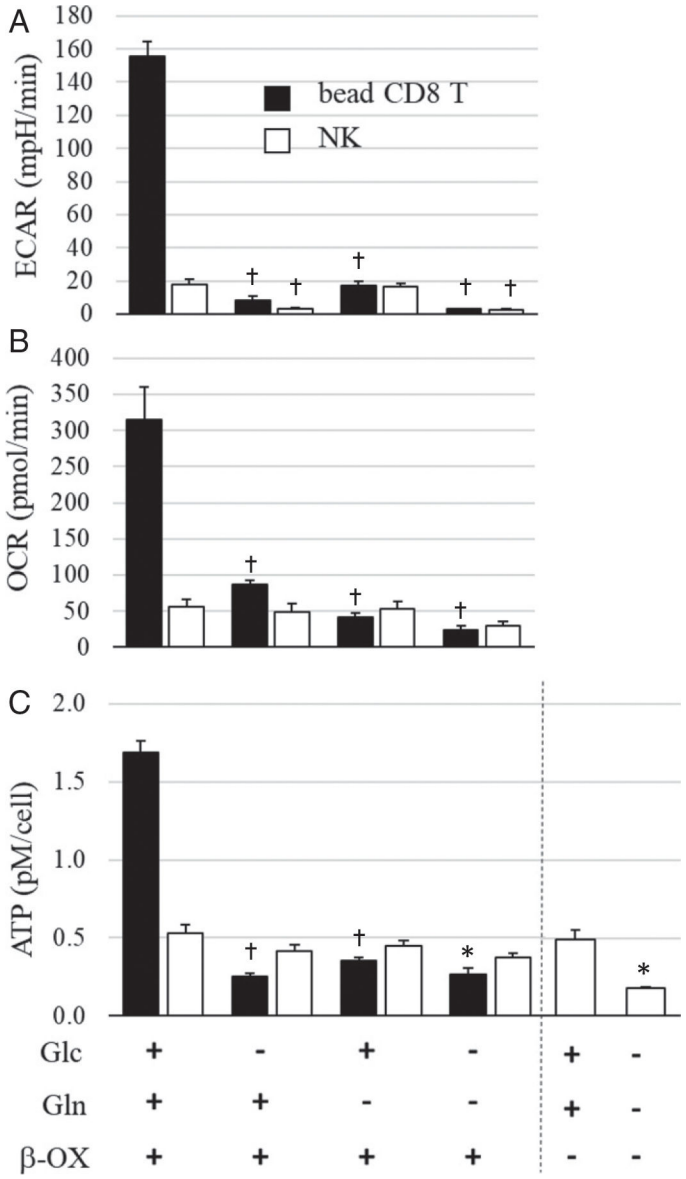

FIGURE 6. Human CD8 T cells require both Glc and Gln for ECAR, OCR, and ATP maintenance, but Gln concentration does not affect human NK cell ECAR, OCR, or ATP level.

Purified cells were activated and stimulated, and ECAR (**A**), OCR (**B**), and ATP, per plated cell (**C**), were measured as described above in cells from six subjects (A and B) or three subjects (C). At initiation, cultures contained 0 or 11 mM Glc and 0 or 2 mM Gln. FA β-oxidation (β-oX) was allowed to proceed (+) or was blocked with 3 μM ETO (−). For this figure, comparison data did not have equivalent variance, and these data were log transformed prior to Student *t* test. $^{*}p < 0.05$, $^{\dagger}p < 0.01$, compared with the 11 mM Glc/2 mM Gln/no ETO condition.

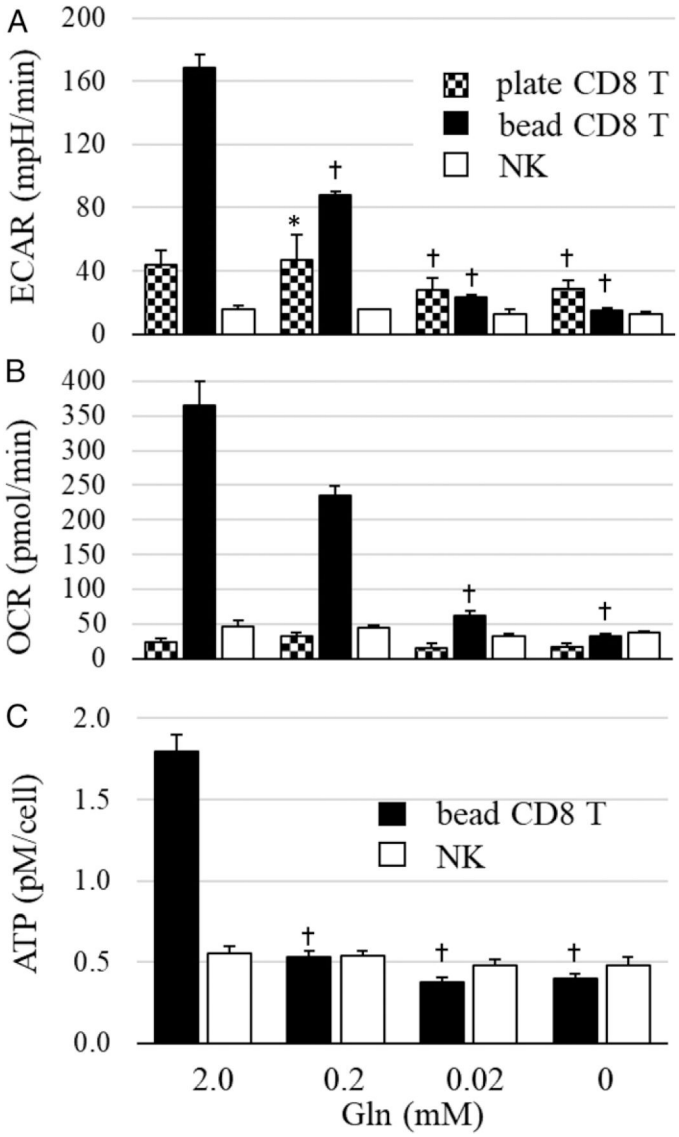

FIGURE 7. Effects of decreasing Gln on CD8 T cell and NK cell metabolism.

Purified cells were activated and stimulated, and ECAR (**A**), OCR (**B**), and ATP, per plated cell (**C**), were measured as described above. At initiation, cultures contained 11 mM Glc, and the Gln concentration indicated on the x-axis. For this figure, comparison data did not have equivalent variance, and these data were log transformed prior to Student *t* test. $^{*}p < 0.05$, $^{\dagger}p < 0.01$, compared with the 2 mM Gln condition within the same cell type generated from four to six subjects (A and B) or three subjects (C).

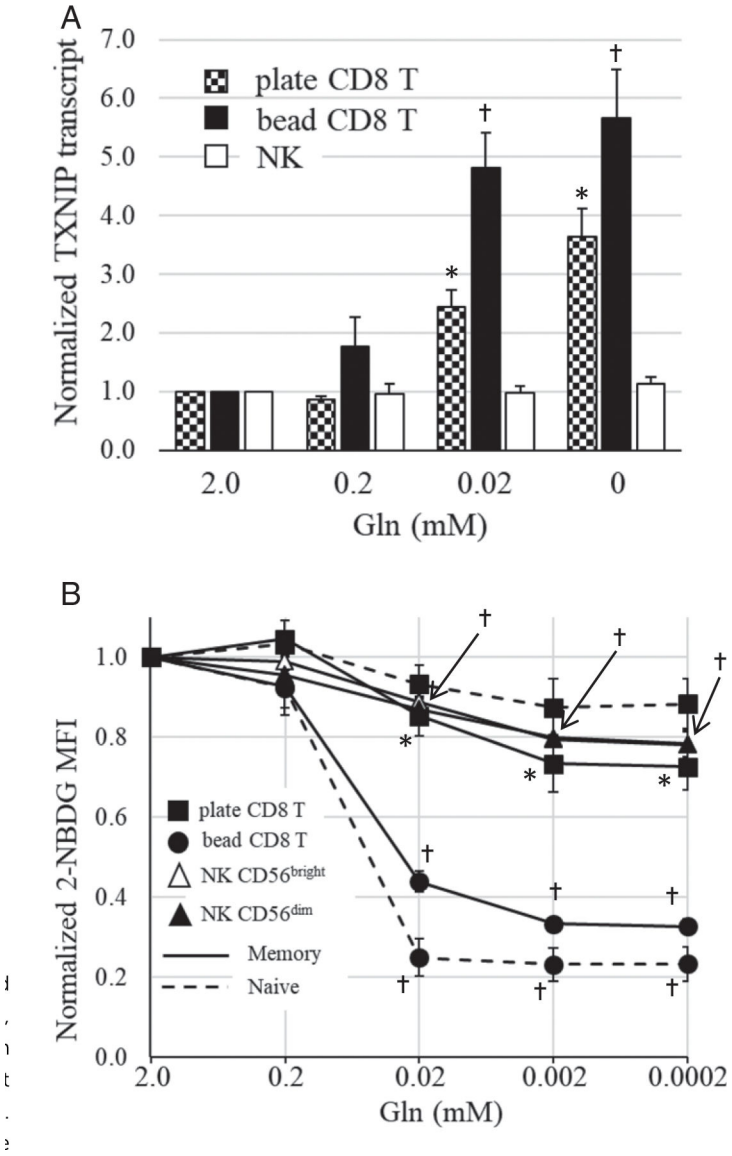

FIGURE 8. Gln suppresses TXNIP expression and increases Glc uptake much more in human CD8 T cells, than in human NK cells.

Purified cells from four or more subjects were activated and stimulated in 11 mM Glc and the indicated Gln concentrations. (**A**) After 2 d, cells were harvested for RNA extraction and quantitative RT-PCR assay, as described in Materials and Methods. (**B**) 2-NBDG uptake was measured by flow cytometry. For 2-NBDG uptake, we distinguished $CD45RA^{+}$ naive CD8 T cells (dashed line) from $CD45RA^{-}$ memory T cells (solid line). Arrows indicate statistical significance for both $CD56^{bright}$ and $CD56^{dim}$ NK cells. $^{*}p < 0.05$, $^{\dagger}p < 0.01$ compared with the 2 mM Gln condition within the same cell type.